Proceedings of 12th IOE Graduate Conference
Peer Reviewed
ISSN: 2350-8914 (Online), 2350-8906 (Print)
Year: 2022 Month: October Volume: 12

Capacity Assessment of Stone Masonry building of Jumla District

Dewakar Acharya [a], Haridarshan Shrestha [b]

[a, b] *Department of Civil Engineering, Pulchowk Campus, IOE, Tribhuvan University, Nepal*
[a] dewakar.acharya@gmail.com, [b] harisunita@gmail.com

Abstract
Located in the colloidal boundary of Indian and Eurasian plates , Nepal lies in the earthquake prone Zone of Nepal. Studies carried out after Gorkha earthquakes 2015 shows that building constructed with stone masonry in mud mortar are highly vulnerable to the earthquakes .Beside shifting of the stress towards western area of Nepal has added the possibility of earthquake of greater magnitude in the western region of Nepal. Jumla district, located in the western regions of Nepal has significant stocks of buildings with stone masonry in the mud mortar. Two storey building with mud roof and two storey with attic floor having CGI sheet cover are most common type of building existing in the Jumla district.
Non linear static analysis of two storey building with attic floor has been carried out in FEM based software Abaqus to obtain the push over curve. Response spectrum curve of Jumla district as specified in NBC 105:2020 and the capacity curve has been used to obtained the performance points(displacement demand). Damaged observed at the performance point (displacement demands) has shown that structure undergoes various damages which includes separation of out of plane gable walls and in plane walls at the attic floor level, shear slides cracks at the footing level and shear failures of in plane walls. Inter storey drift value calculated at the corresponding displacement demand i.e 1.8 % exceeds the limiting values of collapse prevention limit values i.e., 1% as per FEMA 356 which shows that structure are likely to get collapse which conclude that building in Jumla district are highly vulnerable to the earthquakes.

Keywords
Abaqus, push over analysis, Performance point

1. Introduction

Being located at the colloidal boundary of Indian and Eurasian plates,Nepal lies in the zone of high seismicity. Nepal has face several earthquake of magnitude ranging from 6.3 to 8.9 during the various period from 1255 A.D to 2015 A.D.[1]. Studies carried out after the recent Gorkha earthquake 2015[2, 3, 4] highlights that stress built up on the Main Himalayan Thrust fault was partially released in Gorkha earthquakes. It has been believe that some of these stress has shifted towards western area stretching from west of Pokhara, to north of Delhi where no any earthquakes has been recorded since 1505. This additional stress on such seismic gap zone(section with no greater rapture for considerable time) has create greater seismic risk in western region of Nepal.

Experienced from recent Gorkha earthquake (2015) , recorded in PDNA reports[5], 95% (498,852 total houses) of totally destroyed were low strength masonry building(LSM). On the other hand, both observational fragility functions derived by Dipendra Gautam(2018)[6] and analytically derived fragility curve by Rohit K. Adhikari and Dina D'Ayala (2020) [7] for pre earthquake stone masonry in mud mortar (PRE-SMM) typology, highlights that stone masonry buildings of Nepal are highly vulnerable to the earthquakes. All these has create an urgency for the performance evaluation of URM building in mud mortar mainly in western region of Nepal. So study here has been confined to the mud mortar stone masonry in Jumla district of Nepal.

2. Methodology

Methodology adopted in this study has include selection of representative building in first step step. Then literature reviews regarding the analytical approach and material properties has been carried out. Then non linear static pushover analysis to derived force displacement curve has been carried out in next

step. FEM based software Abaqus using macro modelling approach has been selected for fulfillment of this steps. Using this pushover curve and elastic acceleration spectrum from NBC 205:2015[8]as an input data ,N2 method has been used to evaluate the performance level of the selected building.

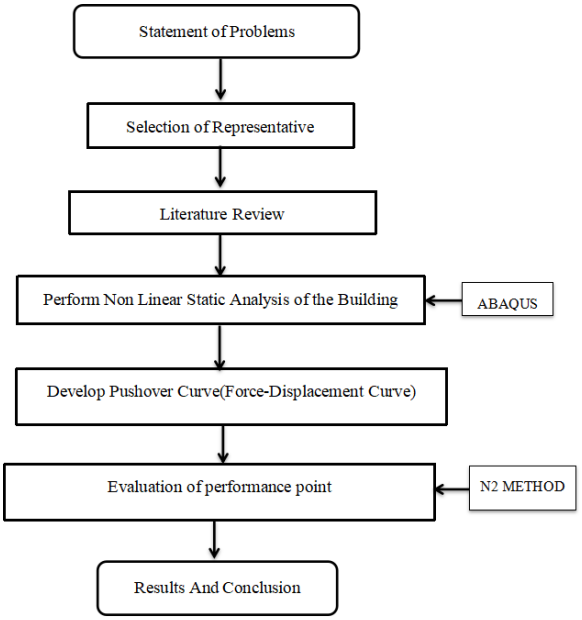

Figure 1: Flowchart of methodology

3. Building in Jumla District

Located in the western region of Nepal Jumla district occupy an area of 2,531 square kilometer of area. As per CBS 2011 report [9] 98.27% of building in Jumla district are mud bonded stone masonry out of which around 87% of building has mud roof while 9% of building has CGI roof cover. Mainly two storey building with mud roof and 2 storey with attic floor having CGI sheet roof cover are common types of building existing in Jumla district. Two storey building with mud roof were constructed either in leveled ground or in sloping ground having step back configuration. Recent trend of addition of CGI roof cover over existing building by adding an attic floor has been noticed in case of Jumla district.

Comparison with the codal provision of NBC 203:2015[8] reveals that lack of vertical bands, large size of opening percentage and improper location of opening specially for door in the internal wall, lack of roof bands, lack of proper connection of roof elements and wall, lack of proper connection of flooring arrangement with the wall, exceed of attic floor height limit are the common structural deficiencies in these buildings. While height of wall,wall thickness,storey height, number of storey,dimension of buildings ,unsupported wall length existing in buildings t has found to satisfy the codal provision. Provision of minimal to maximum horizontal bands are another key characteristics of building existing in Jumla district. Two storey building with attic floor having CGI sheet roof cover has been considered for this study.

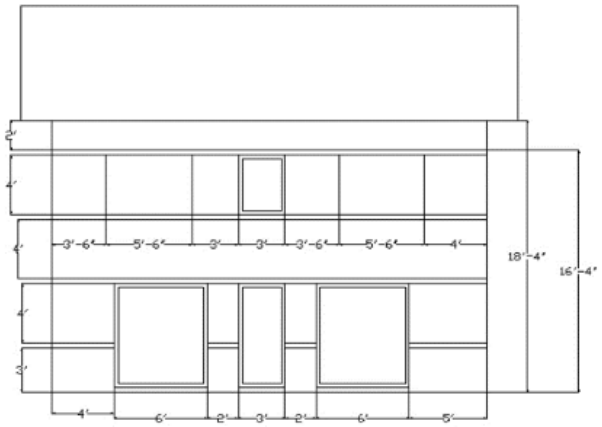

Figure 2: Front elevation

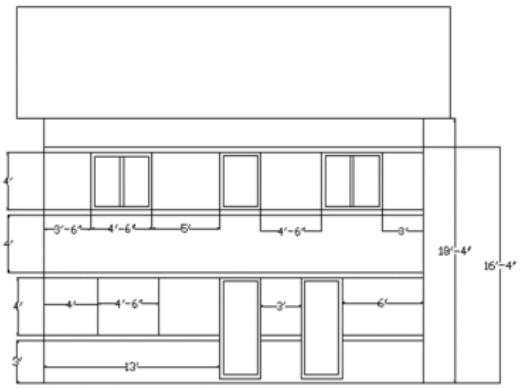

Figure 3: Back Elevation

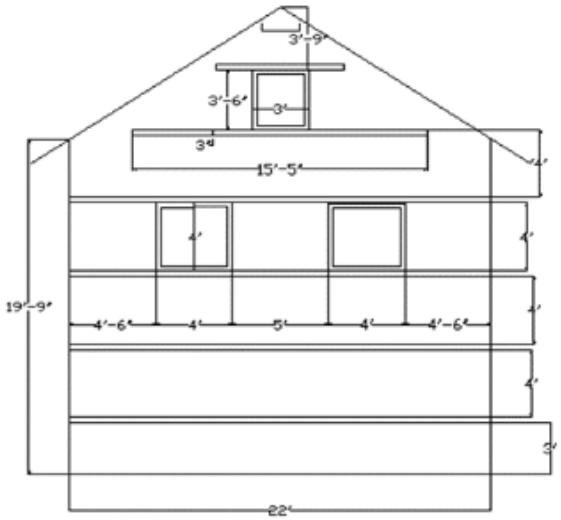

Figure 4: Side Elevation

Figure 7: Attic floor plan

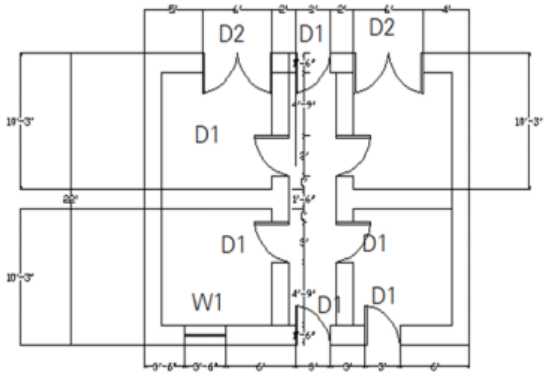

Figure 5: Ground floor plan

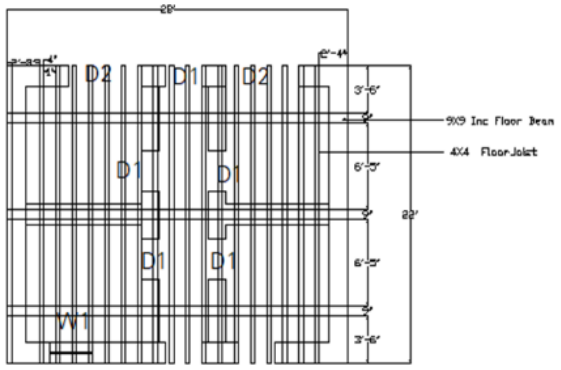

Figure 8: Arrangements of beams and joist in first floor

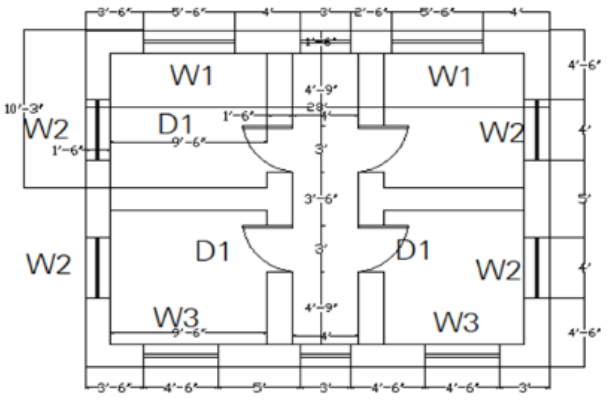

Figure 6: second floor plan

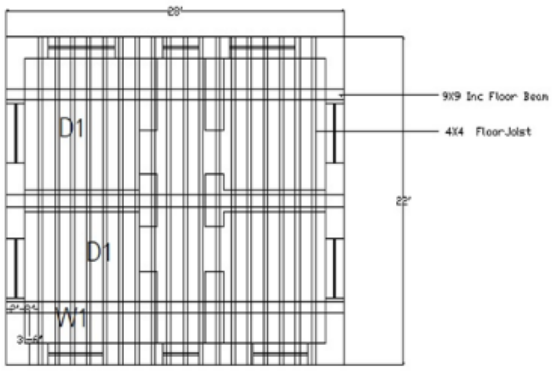

Figure 9: Arrangements of beams and joist in second floor

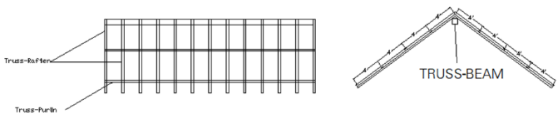

Figure 10: Purlin and rafter arrangements

4. Modelling and Analysis

4.1 Fem Modelling in ABAQUS

Three-dimensional finite element is the most prominent method that has been used in modeling the masonry building[10, 11, 12, 13, 14, 15]. In finite element method three approaches are popular i.e., micro element modeling, simplified micro element method and macro element modeling method[16]. Micro modelling approach which considered the masonry as homogeneous elements has been used in this study , as computational time required for micro and simplified micro element are relatively higher similar approach to model the masonry building can be found in various literature [10, 11, 12, 13, 14, 15].

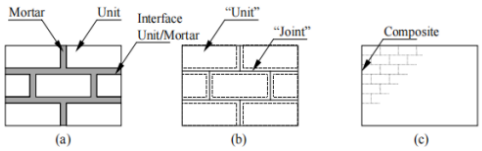

Figure 11: Various modelling approaches in FEM (a) Micro modelling, (b)simplified micro element modelling and (c)macro element method

Three dimensional 8 nodded hexahedral element with reduced integration(3CD8R) has been used to model the both masonry and timber elements. Floor beam ,floor joist,horizontal bands ,rafter and purlin has been included in the model. While CGI sheet ,broken pieces of planks and mud laid over the floor joist has been excluded in the model. However dead load contributed by them has been taken into account by increasing the density of floor joist and roof purlin. Purlin,rafter and ridge beam which has been been connected together by the nail has been modeled as an single integrated element to meets the purpose of load transfer from this member to peripheral wall similar way of modelling the purlin and rafter can be found in [13, 14, 15]. In case of building in Jumla district , floor joist are simply laid on floor beams and all floor joist,floor beam and ridge beam are laid on the masonry wall upto full or half thickness of wall. While rafter has been found to simply rest on wall. No special provision for their connection with wall has been found. To model this hole has been created upto full or half thickness of wall in which main beam,floor joist and ridge beam has been laid on their respective hole. Hard contact for the normal transfer of force and frictional approach using coefficient of 0.6[17] for tangential transfer of force has been used in this modelling approach similar approach of contact modelling can be found in various literature[18, 19]. Timber bands has been modeled as embedded elements in which works in similar manner as reinforcement bars in concrete reinforcement[20],modelling of bands in similar manner can be found in the literature[10]. After creating this model various material property has been assigned for the respective elements.

Figure 12: C3D8R element (Adopted from abaqus manual)

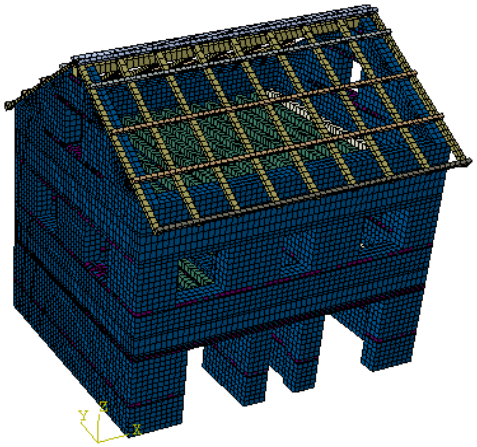

Figure 13: Finite Element Model of the considered building in Abaqus

4.2 Material Property

Roof arrangement,band,floor beam and floor joist being made of wooden element has been model as a linear element. Parameter to defined such linear elements includes density,Poisson's ratio and young modulus of elasticity. Density and Young Modulus of elasticity has been taken from NBC 112:1994[21] consider sal wood while Poisson ratio has been taken

from relevant literature as shown below.

Table 1: Property Of Timber elements

Material Property	Value	Source
Density	865 kg/m³	NBC 112:1994[22]
Modulus of elasticity	12500 KN/mm²	NBC 112:1994[22]
Poisson ratio	0.3	Parajuli, 2016[23]

Adopted modelling approach excludes CGI sheets ,pieces of plank and mud existing in flooring arrangement and roof arrangement respectively. However they contribute dead load in the system. For this unit weight has been taken from the IS 875 (Part-1):1987[7]and corresponding load has been distributed in rafter and floor joist by increasing their density. Table below shows the density of these elements

Table 2: Property of CGI sheet and mud floor

Material Property	Value	Source
Unit weight of mud	14.10 KN/m³	IS 875 (Part-1): 1987[7]
Unit weight of CGI Sheet	5.5 Kg/m²	IS 875 (Part-1): 1987[7]

Masonry elements has been modeled as non linear elements. Both elastic and plastic property are needed to be defined. Elastic property to be defined for the masonry elements which include density,modulus of elasticity has been adopted from Table 3 shown below. While Poisson ratio has been taken to be 0.2 from Parajuli (2016)[23].

Table 3: Materials properties for Nepalese rubble stone masonry in mud mortar (Build Change,2019) (Adopted from Adhikari and Ayala (2020))

Material Property	Average Value	CoV (%)
Unit Weight	2200 kg/m³	
Young's Modulus	65.10 MPa	31
Shear Modulus	22.40 MPa	
Compressive Strength	2.40 MPa	13
Tensile strength	0.02 MPa	16.5
Cohesion	0.013 MPa	16.5
Coefficient of friction	0.40	

To model the plastic behaviour of the masonry elements damage plasticity (CDP) constitutive law ,suitable for the quasi brittle elements ,has been adopted in the model. Use of similar constitutive law for modelling of URM can be found in various literature [11, 12, 13, 14, 15]. CDP model adopted in this study assumes two failure mechanisms i.e., tensile cracking and compressive crushing of the concrete material[20]. The evolution of the yield (or failure) surface in such model is controlled by two hardening variables i.e., tensile equivalent plastic strain and compressive equivalent plastic strain, linked to failure mechanisms under tension and compression loading, respectively. The model assumes that the uni-axial tensile and compressive response characterized by the damage plasticity as shown in the figure below. The degradation of the elastic stiffness is characterized by two damage variables, dc and dt for compression and tension respectively, and their evolution is a function of the plastic strains.

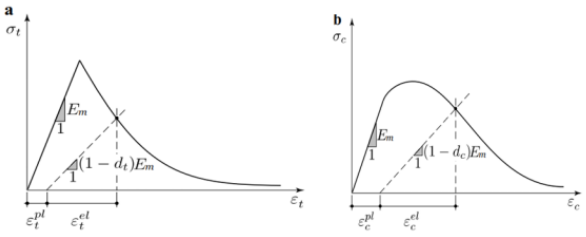

Figure 14: Response in (a)uni axial tension and (b)uni axial compression

$$\sigma_t = (1-d_t)E_m(\varepsilon_t - \varepsilon_t^{pl}) \quad (1)$$

$$\sigma_c = (1-d_c)E_m(\varepsilon_t - \varepsilon_t^{pl}) \quad (2)$$

Where

E_m=Undamaged Elastic Modulus

d_t,d_c =Damage Variable in tension and compression

ε_t = Total strain in tension

ε_c = Total strain in Compression

ε_t^{pl} = equivalent plastic strain component in tension

ε_c^{pl} = equivalent plastic strain component in compression

A simplified ti-linear curve proposed by Akhaveissy et al. [24] for tensile behaviour and parabolic curve purposed by Naraine, K. and Sinha, S [25] has been used to generate the stress strain curve in tension and

compression respectively. Tensile strength , compression strength and modulus of elasticity required to generate these curve has been adopted from Table 3. Use of similar curve in case of mud bonded stone masonry can be found in [13].

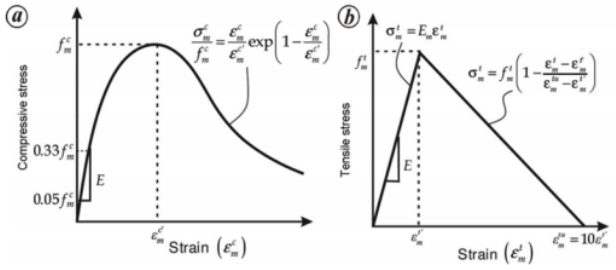

Figure 15: Compressive behaviour cure(a) and tensile behaviour curve(b) Proposed by [27-28]

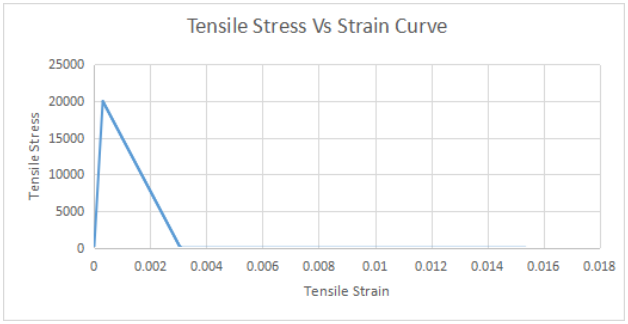

Figure 16: Tensile stress -strain curve used in this study

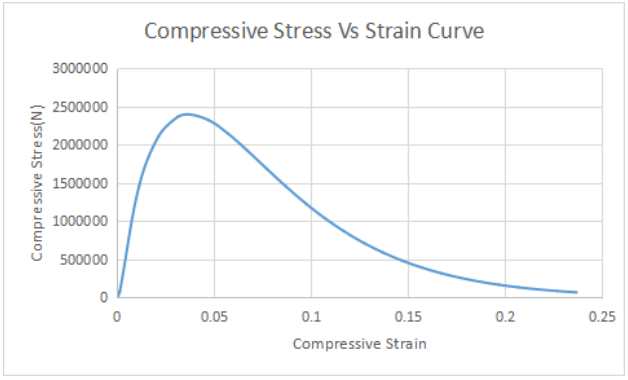

Figure 17: Compressive stress-strain curve used in this study

Yield stress,tensile cracking strain ,compressive inelastic strain and damage variables to be input for the CDP model has been calculated using the curve (a) and (b) using the following relationship. Cracking strain for any yield stress= Strain at that yield stress in curve-elastic strain

Inelastic strain for any yield stress= Strain at that yield stress in curve-elastic strain

$$Elastic\ \ strain = \frac{Yeild\ \ Stress}{Young's\ \ Modulus} \tag{3}$$

$$Damage\ variable(dt) = 1 - \frac{Yeild\ \ Stress}{Tensile\ \ Strength} \tag{4}$$

However in case of the compressive curve as the yield stress doesn't varies linearly with strain so the equivalent energy concept [26] has been used to define the damage parameter (dc)as illustrated in the figure below.

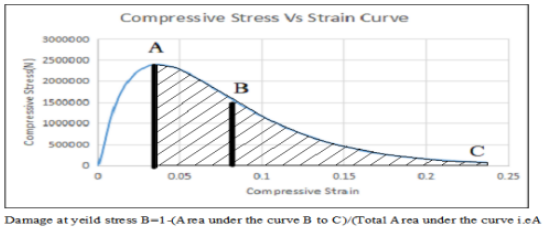

Figure 18: Compressive damage parameter used in this study

Table 4: Tensile properties used in Abaqus

Yield Stress	Cracking Strain	Damage
20000	0	0
19349	0.0001	0.03255
18698	0.0002	0.0651
18047	0.0003	0.09765
17830	0.000333333	0.1085
17613	0.000366667	0.11935
17396	0.0004	0.1302
17179	0.000433333	0.14105
16962	0.000466667	0.1519
16745	0.0005	0.16275
16528	0.000533333	0.1736
16094	0.0006	0.1953
15660	0.000666667	0.217
15443	0.0007	0.22785
15226	0.000733333	0.2387
15009	0.000766667	0.24955
14792	0.0008	0.2604
14575	0.000833333	0.27125
12188	0.0012	0.3906
10235	0.0015	0.48825
1338	0.002866667	0.9331
1121	0.0029	0.94395
904	0.002933333	0.9548
687	0.002966667	0.96565
470	0.003	0.9765
36	0.003066667	0.9982

Table 5: Compression properties used in Abaqus

Yield Stress	Inelastic Strain	Damage
2400000	0	0
2326161.318	0.011134235	0.030766118
2151947.431	0.023810331	0.103355237
1929219.009	0.037231659	0.196158746
1690860.537	0.050893079	0.295474776
1456869.724	0.064487408	0.392970948
1238624.588	0.077839868	0.483906421
1041850.383	0.090862513	0.565895674
868663.3095	0.103522837	0.638056954
718962.2075	0.115822393	0.700432414
591362.6916	0.127782447	0.753598879
483812.5813	0.139434523	0.798411424
393987.3406	0.150814327	0.835838608
319535.3146	0.161957983	0.866860286
258221.8154	0.172899819	0.892407577
208006.2766	0.183671179	0.913330718
167076.1455	0.194299906	0.930384939
133853.7154	0.204810235	0.944227619
106986.8423	0.215222936	0.955422149
85330.81711	0.225555594	0.964445493

Apart from mentioned above various other parameters parameter that are required to define the plasticity for CDP and their sources has been highlighted below

Table 6: Parameters adopted to define plastic Properties

Property	Value	Source
The distance from the hydro static axis of the maximum compression and tensile stress(Kc)	0.667	Abaqus (2014)
Dilatation angle	30°	Rai et.al (2016)[13]
Ratio between the bi-axialand mono-axial compression strength(fb0/fc0)	1.16	Rai et.al(2016)[13]
Flow potential eccentricity (ε)	0.1	Default Value in Abaqus, Rai et.al (2016)[13]
Viscosity parameter	0.0001	Rai et.al (2016)[13]

4.3 Boundary Condition and Loading

Fixed support has been assumed at the base.While gravitational load has been applied in first step and then mass proportional lateral load has been applied in subsequent steps.

5. Analysis and Results

5.1 Pushover Analysis

Analysis has been carried out by applying the monotonically increasing later load in +X, -X, +Y and -Y direction and pushover curve has been obtained by plotting base shear vs roof drifts as shown below.

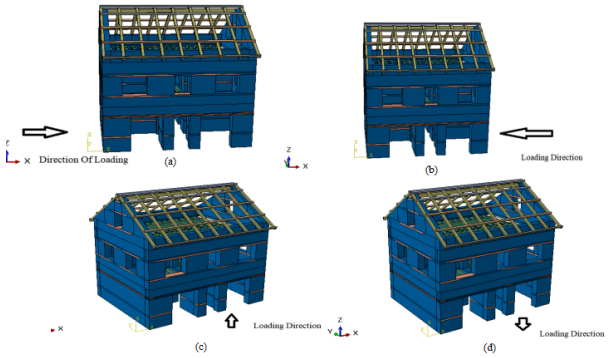

Figure 19: Pushover analysis of builing in (a) + X dir,(b)-X dir ,(c)+Y dir and (d)-Y dir

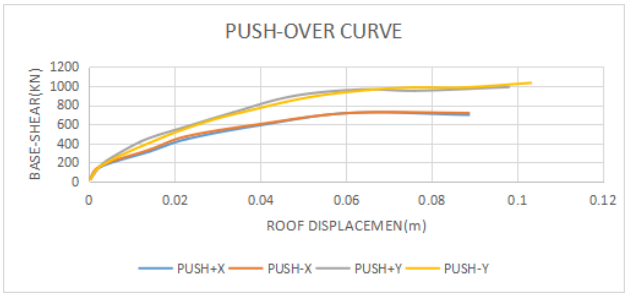

Figure 20: Pushover curve

Pushover curve obtained above shows that push in X direction is the critical direction of loading. Capacity curve to evaluate the permanence points has been carried out by using the Push over curve in +X direction of loading.

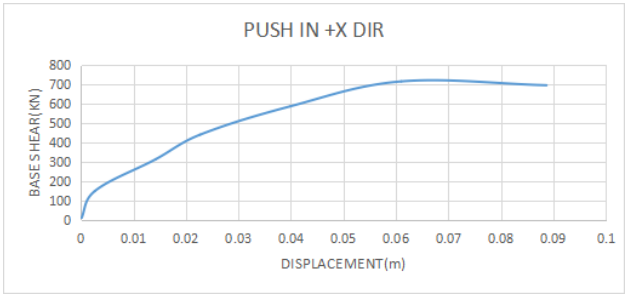

Figure 21: Pushover curve for critical direction of loading

5.2 Application of N2 Method

Elastic acceleration spectrum of Jumla district obtained from NBC 105:2020[22] has been converted into elastic spectrum in acceleration displacement format. Where

$$Sde = \frac{T^2}{4\pi^2} Sa \tag{5}$$

Where Sde=Spectral displacement, Sae=Spectral acceleration and T= Time Period

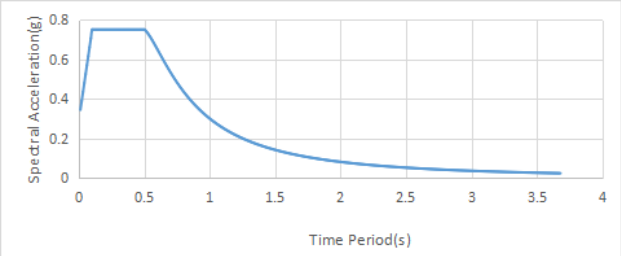

Figure 22: Acceleration spectrum curve for Jumla district

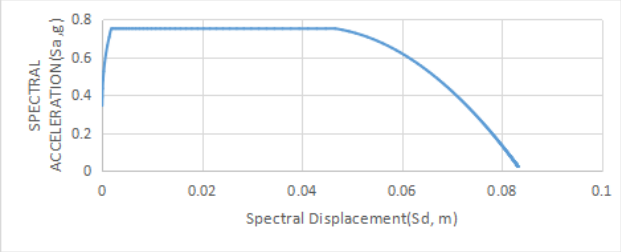

Figure 23: Acceleration spectrum curve in spectral acceleration-Displacement format

MDOF push over curve has been converted into equivalent SDOF capacity curve by transforming the MDOF quantities to SDOF quantities using the following relationship.

$$Spectral\ \ Acceleration(Sa) = \frac{F}{\Gamma * m^*} \tag{6}$$

$$m^* = \Sigma m_i * \Phi_i \tag{7}$$

$$\Gamma = \frac{(\Sigma m_i * \Phi_i)}{\Sigma m_i * {\Phi_i}^2} \tag{8}$$

$$Spectral\ \ Displacement(Sd) = \frac{D}{\Gamma} \tag{9}$$

where

m_i=Lumped mass at floor level

$\Phi_i = Displacement at ith floor$

$\Gamma = 1.7356$

m^*=146473.208 kg

$$T^* = 2\pi\sqrt{(\frac{m^* * D_y}{F_y})} \tag{10}$$

T^*=0.696sec

Using the above parameters capacity curve and performance points has been evaluated shown below.

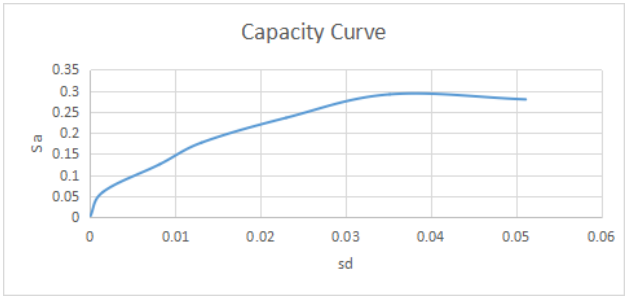

Figure 24: Capacity curve for building

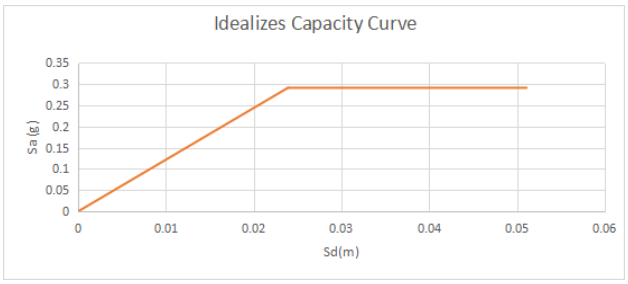

Figure 25: Bilinearized capacity curve

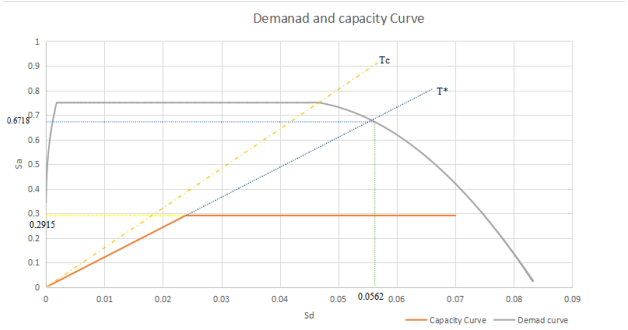

Figure 26: Evalution of performance points using capacity curve and demand curve

From the Figure 28

$$Reduction\ \ factor(R\mu) = (\frac{Sae}{Say}) \tag{11}$$

$Reduction\ \ factor(R\mu) = 2.304$

$SinceT* \geq Tc$

Sd=Se=0.0562

$Displacement demand for the MDOF system = \Gamma x Sd = 0.09754m$

5.3 Damage Observation

Tensile damage pattern has been observed at the corresponding displacement demands. Tensile damage are observed whenever the tensile stress exceeds the tensile strength at particular region of the building. Observed vertical pattern of tensile damage signifies that in plane and out of plane wall tends to separate from each other at the attic floor level. While observed horizontal tensile damages signifies slide shear damages at the footing level. Diagonal damages on the in plane walls shows that due to presence of horizontal seismic bands diagonal shear has been utilized for the resistance of earthquake force. Inter storey drift has been found to be 1.8% which exceeds the limiting values of collapse prevention limits i.e., 1% as per FEMA 356[27].

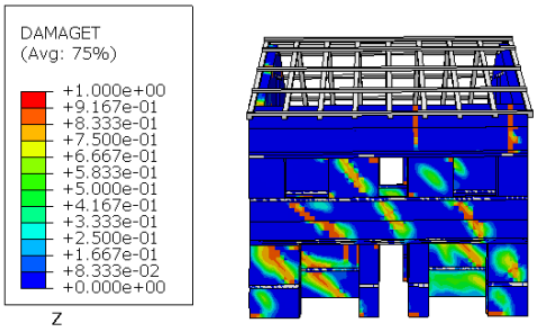

Figure 27: Damage in front face at demand displacement

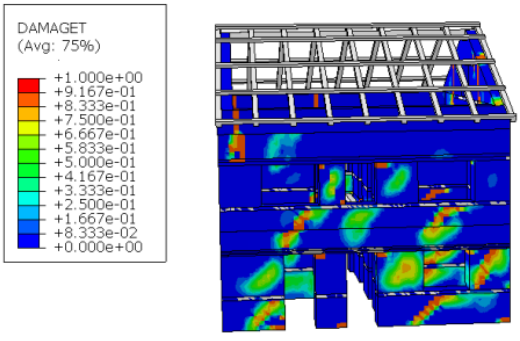

Figure 28: Damages in the back face

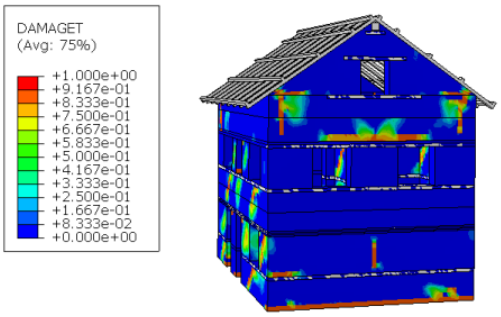

Figure 29: Damage in side faces at demand diplacement

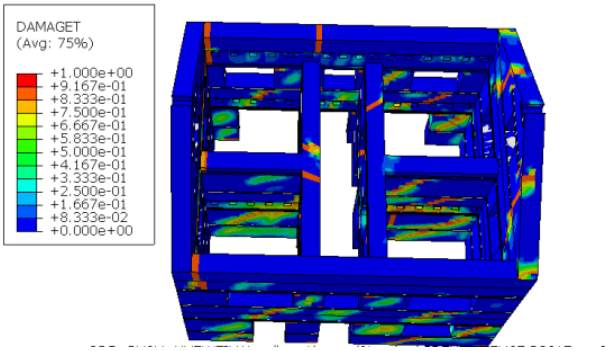

Figure 30: Damages in the internal walls

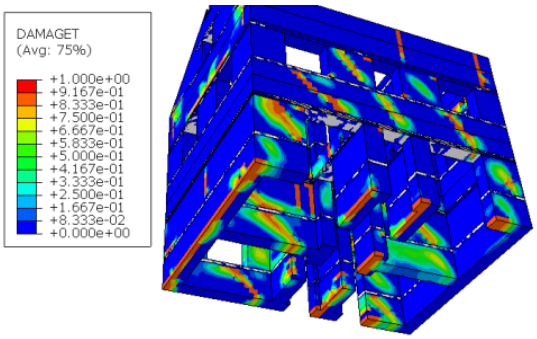

Figure 31: Damages in the walls bases

6. Conclusion

Building with gable present in the Jumla district has been analyzed using the finite element method using homogeneous macro modelling approach in the Abaqus. Non linear static analysis has been carried out using the concrete damage plasticity constitutive law. Response spectrum curve of Jumla district as specified in NBC 105:2020[22] and capacity curve from pushover analysis has been used to evaluate the performance points using N2 methods. Demand roof displacement for such type of building has been found to be 0.09754m. Damages observed at the

corresponding roof displacements shows that building undergoes extensive damages, calculated maximum inter strorey drift limit has been observed to be 1.8% which exceed the collapse prevention inter storey drift limits (1%) as specified in FEMA 356[27] which conclude that such buildings are highly vulnerable to the earthquakes.

References

[1] https://en.wikipedia.org/wiki/List of earthquakes in Nepal.

[2] https://www.bbc.com/news/science-environment-33807791.

[3] https://reliefweb.int/report/nepal/kathmandu-not-most-risk-earthquakes.

[4] 4.https://www.air-worldwide.com/blog/posts/2015/5/did-the-nepal-earthquake-close-the-gap/.

[5] GON. *Post Disaster Needs Assessment(PDNA),Volume B*.

[6] Dipendra Gautam, Giovanni Fabbrocino, and Filippo Santucci de Magistris. Derive empirical fragility functions for nepali residential buildings. *Engineering Structures*, 171:617–628, 2018.

[7] *IS 875 (Part-1): 1987*.

[8] *NBC203:2015*.

[9] Central Bureau of Statistics (CBS). *6.National population and housing census (national report). Kathmandu: Government of Nepal; 2011. p. 2012*.

[10] Dimitris Dais, Vasilis Sarhosis, Eleni Smyrou, and Ihsan Engin Bal. Seismic intervention options for multi-tiered nepalese pagodas: The case study of jaisedewal temple. *Engineering Failure Analysis*, 123:105262, 2021.

[11] Giovanni Castellazzi, Antonio Maria D'Altri, Stefano de Miranda, Andrea Chiozzi, and Antonio Tralli. Numerical insights on the seismic behavior of a non-isolated historical masonry tower. *Bulletin of Earthquake Engineering*, 16(2):933–961, 2018.

[12] Mirko Pejatovic, Vasilis Sarhosis, and Gabriele Milani. Multi-tiered nepalese temples: advanced numerical investigations for assessing performance at failure under horizontal loads. *Engineering Failure Analysis*, 106:104172, 2019.

[13] Durgesh C Rai, Vaibhav Singhal, Tripti Pradhan, and Anu Tripathi. Seismic vulnerability of monastery temples of stone masonry in sikkim himalaya. *Curr. Sci*, 110(10):1947–1957, 2016.

[14] Michele Betti and Luciano Galano. Seismic analysis of historic masonry buildings: the vicarious palace in pescia (italy). *Buildings*, 2(2):63–82, 2012.

[15] Emre Ercan, Bengi Arisoy, Emin HÖKELEKLİ, and Ayhan NUHOĞLU. Estimation of seismic damage propagation in a historical masonry minaret. *Sigma Journal of Engineering and Natural Sciences*, 35(4):647–666, 2017.

[16] Jan Gerrit Rots. *Structural masonry: an experimental/numerical basis for practical design rules*. CRC Press, 1997.

[17] João P Almeida, Katrin Beyer, Roland Brunner, and Thomas Wenk. Characterization of mortar–timber and timber–timber cyclic friction in timber floor connections of masonry buildings. *Materials and Structures*, 53(3):1–14, 2020.

[18] Ornella Iuorio and Jamiu A Dauda. Retrofitting masonry walls against out-of-plane loading with timber based panels. *Applied Sciences*, 11(12):5443, 2021.

[19] Kyriazis Pitilakis, Stella Karafagka, Olga Ntinoudi, Ioannis S. Kalogeras, Vasiliki, and Eleftheriou. Seismic hazard analysis of the acropolis of athens and seismic analysis of propylaea colonnade. 2018.

[20] *Abaqus analysis user's manual(V6.6)*.

[21] *NBC 112:1994*.

[22] *NBC105:2020*.

[23] Hari Ram Parajuli. Performance of mud bonded stone masonry houses and mitigation. *Nepal Journal of Science and Technology*, 17(1):27–30, 2016.

[24] Amir H Akhaveissy and Chandrakant S Desai. Unreinforced masonry walls: Nonlinear finite element analysis with a unified constitutive model. *Archives of Computational Methods in Engineering*, 18(4):485–502, 2011.

[25] Krishna Naraine and Sachchidanand Sinha. Cyclic behavior of brick masonry under biaxial compression. *Journal of Structural Engineering*, 117(5):1336–1355, 1991.

[26] Nina Zheng, Jing Zhou, Yuanyuan Yin, Jun Han, and Shuyan Ji. Non-linear time history response analysis of low masonry structure with tie-columns. In *Fifteenth World Conference on Earthquake Engineering, Lisboa*, 2012.

[27] *FEMA356*.